# Outer Approximation of Attractors Using an Interval Quantization*

Luc Jaulin
Lab-STICC, IHSEV, OSM, ENSTA-Bretagne
Brest, France
luc.jaulin@ensta-bretagne.fr

**Abstract**

An attractor is the set toward which the solutions of a dynamical system converge. In this paper, the system is described by an autonomous state equation of the form $\dot{\mathbf{x}} = \mathbf{f}(\mathbf{x})$. When the function $\mathbf{f} : \mathbb{R}^n \to \mathbb{R}^n$ is nonlinear, interval analysis is needed to provide a guaranteed conclusion. Existing interval-based methods cover the state space with small boxes and perform an interval integration for each of them, which makes the technique limited to small dimensional problems. This paper shows that an outer approximation of attractors can be built without any interval integration. The concept is to perform a quantization of the state equation into a dynamical graph. The nodes of this graph are polytopes covering the state space. A test case related to the station keeping of a non-holonomous robot illustrates the principle of the approach.

**Keywords:** attractors, graph, interval analysis, limit sets, robotics.

## 1 Introduction

We consider a dynamical system described by the state equation

$$\dot{\mathbf{x}} = \mathbf{f}(\mathbf{x}), \tag{1}$$

where $\mathbf{x} \in \mathbb{R}^n$ is the state vector, and $\mathbf{f} : \mathbb{R}^n \to \mathbb{R}^n$ is a nonlinear function. For simplicity, we assume that the state space corresponds to $\mathbb{R}^n$, but the approach easily extends to manifolds locally equivalent to $\mathbb{R}^n$. We also assume that, for any initial vector $\mathbf{x}_0 \in \mathbb{R}^n$, the state equation has a unique solution denoted by $\phi(t, \mathbf{x}_0)$. It is the case, for instance, if $\mathbf{f}$ is locally Lipschitz. The *limit set* [1] of the system is defined by

$$\mathbb{X}^\infty = \{\mathbf{x} \in \mathbb{R}^n \text{ s.t. } (\forall \varepsilon \in ]0,1]) \ (\exists t \in ]1,\infty[) \ (\|\phi(t,\mathbf{x}) - \mathbf{x}\| < \varepsilon)\}.$$

*Submitted: February 6, 2013; Revised: March 23, 2014; Accepted: April 2, 2014.

This limit set may enclose unstable subsets of $\mathbb{R}^n$, but it always contains the attractor of the system (i.e., the set to which the system converges when $t$ tends to infinity). Interval analysis [15, 17] has been used by several authors to characterize attractors [6, 26] or capture basins [13]. The problem has also strong similarities with the characterization of reachable sets [3, 20, 21], which also can be studied efficiently with interval-based methods. All these methods require bisecting the state space into small boxes and integrating the state equation for all these small boxes. This makes these approaches limited to very small dimensional problems (i.e., $n \leq 4$). Note that there exist also point methods to tackle this type of problems [4, 22], but they require some Lipschitz assumptions that are rarely available, and they also suffer from the same drawbacks with respect to the dimension of the problem.

The problem to be considered in this paper is to provide an outer approximation of the limit set (or the attractor) of a dynamical system. The method does not requires any interval integration [2, 16] of the system. The main idea is to decompose the state space with polytopes and to build a graph the nodes of which correspond to the polytopes.

The paper is organized as follows. Section 2 provides the theoretical notions that are required to quantize our problem into a problem involving discrete graphs. Section 3 presents an original example of station keeping. The corresponding test case can be cast into a two-dimensional problem and allows a graphical representation of the dynamics of the system. Section 4 illustrates the method on this simple example. Section 5 concludes the paper.

## 2 Quantization

This section provides some basic notions which are required to build a discrete dynamical graph from the state equation (1). This operation can be interpreted as a tiling of the state space and thus will be called a *quantization* (the word *discretization* that could also have been used is generally devoted to a time mincing). The quantization is based on interval analysis to guarantee properties of the initial dynamical system. The principle of using interval analysis for quantizing a continuous problem into a graph has already been used for path planning [8, 19] or to analyze the topology of set defined by nonlinear inequalities [5]. In the paper, the same principle will be applied, except that here, a differential equation is involved.

**Paving.** A paving (see e.g., [23]) of the state space $\mathbb{R}^n$ is a collection $\Omega = \{\mathbb{X}_1, \mathbb{X}_2, \ldots, \mathbb{X}_p\}$ of non-overlapping polytopes $\mathbb{X}_i$ such that

$$\bigcup_{i=1}^{p} \mathbb{X}_i = \mathbb{R}^n.$$

**Relation**. Consider a point $\mathbf{x}_0 \in \mathbb{X}_i$. We define the time $\eta_i(\mathbf{x}_0)$ at which the system leaves $\mathbb{X}_i$ for the first time, *i.e.*,

$$\eta_i(\mathbf{x}_0) = \inf\{(t \in ]0, \infty[) \ (\phi(t, \mathbf{x}_0) \notin \mathbb{X}_i)\}. \tag{2}$$

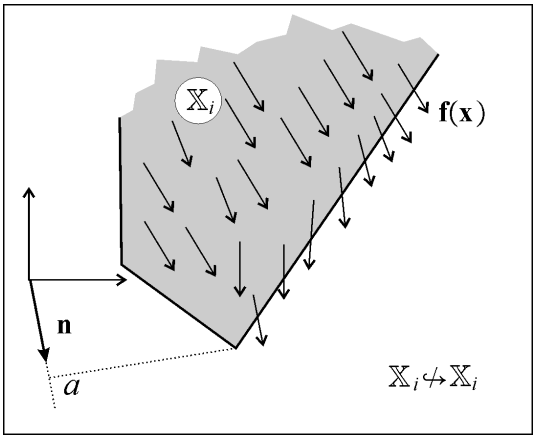


Figure 1: Since all trajectories inside the polytope $\mathbb{X}_i$ will escape $\mathbb{X}_i$, we have $\mathbb{X}_i \not\hookrightarrow \mathbb{X}_i$.

Consider two polytopes $\mathbb{X}_i$ and $\mathbb{X}_j$ of $\Omega$. We define the relation $\hookrightarrow$ between $\mathbb{X}_i$ and $\mathbb{X}_j$ as follows

$$(\mathbb{X}_i \hookrightarrow \mathbb{X}_j) \Leftrightarrow \begin{cases} \text{(i)} & (\exists \mathbf{x}_0 \in \mathbb{X}_i) \quad (\phi(\eta(\mathbf{x}_0), \mathbf{x}_0) \in \mathbb{X}_j) \\ \text{(ii)} & \dim(\mathbb{X}_i \cap \mathbb{X}_j) \geq n-1. \end{cases} \tag{3}$$

The first condition (i) tells us that the trajectory can cross the common frontier $\mathbb{X}_i \cap \mathbb{X}_j$ from $\mathbb{X}_i$ to $\mathbb{X}_j$. Condition (ii) requires that the polytope $\mathbb{X}_i$ and $\mathbb{X}_j$ intersect each other, but not only on the corner: If the polytope $\mathbb{X}_i \cap \mathbb{X}_j$ has a dimension equal $n-1$, then $\mathbb{X}_i$ and $\mathbb{X}_j$ are bonded to each other through their common face; If $\dim(\mathbb{X}_i \cap \mathbb{X}_j) = n$, then we should have $\mathbb{X}_i = \mathbb{X}_j$.

**Convention.** If there exists $\mathbf{x}_0 \in \mathbb{X}_i$, such that $\forall t > 0, \phi(t, \mathbf{x}_0) \subset \mathbb{X}_i$, then $\eta(\mathbf{x}_0) = \infty$. In this situation, we could write $\phi(\eta(\mathbf{x}_0), \mathbf{x}_0) \in \mathbb{X}_i$, and we shall consider that $(\mathbb{X}_i \hookrightarrow \mathbb{X}_i)$.

**Quantization**. A *quantization* of the state equation (1) is a graph $\mathcal{G}$ (*i.e.*, a subset of $\Omega \times \Omega$) defined by

$$(\mathbb{X}_i, \mathbb{X}_j) \in \mathcal{G} \Leftrightarrow \mathbb{X}_i \hookrightarrow \mathbb{X}_j.$$

The quantization will by denoted by $\mathcal{G} = (\Omega, \hookrightarrow)$.

**Proposition 1**. Consider a polytope $\mathbb{X}_i$ of $\Omega$, a vector $\mathbf{n}$ and two real numbers $\varepsilon < 0$ and $a \in \mathbb{R}$. We have

$$((\forall \mathbf{x} \in \mathbb{X}_i) \quad ((\mathbf{n}^{\mathrm{T}} \cdot \mathbf{f}(\mathbf{x}) \geq \varepsilon) \ \wedge \ (\mathbf{n}^{\mathrm{T}} \cdot \mathbf{x} \leq a))) \Rightarrow (\mathbb{X}_i \not\hookrightarrow \mathbb{X}_i).$$

**Proof.** The proof is by contradiction and is illustrated by Figure 1. Define the function $V(t) = \mathbf{n}^{\mathrm{T}} \cdot \mathbf{x}(t)$ and assume that for all $t > 0$, $\mathbf{x}(t) \in \mathbb{X}_i$. We have

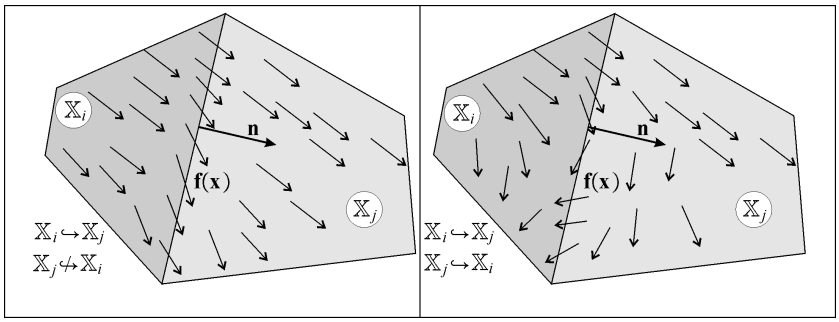


Figure 2: Interpretation of the relations $\hookrightarrow$ and $\not\hookrightarrow$

$\dot{V}(t) = \mathbf{n}^{\mathrm{T}} \cdot \mathbf{f}(\mathbf{x}) \geq \varepsilon > 0$, and thus $V(t)$ converges to $+\infty$. This is inconsistent with the fact that $\mathbf{n}^{\mathrm{T}} \cdot \mathbf{x} \leq a$. ■

**Test 1.** Consider a set $\mathbb{X}_i$ of $\mathbb{R}^n$ and take any $\mathbf{v}$, *e.g.*, $\mathbf{v} = -\mathbf{f}(\mathbf{x}_0)$, where $\mathbf{x}_0 \in \mathbb{X}_i$. Take a box $[\mathbf{x}]$ enclosing $\mathbb{X}_i$. The lower bound of $\mathbf{v}^{\mathrm{T}} \cdot [\mathbf{x}]$ corresponds to $a$. Using interval computation, we can check that $\mathbf{v}^{\mathrm{T}} \cdot \mathbf{f}(\mathbf{x})$ is strictly negative in $\mathbb{X}_i$. If it is the case, we conclude that $\mathbb{X}_i \not\hookrightarrow \mathbb{X}_i$.

**Proposition 2**. Consider two polytopes $\mathbb{X}_i$ and $\mathbb{X}_j$ of $\Omega$ and assume that $\dim(\mathbb{X}_i \cap \mathbb{X}_j) = n - 1$ (i.e., $\mathbb{X}_i$ and $\mathbb{X}_j$ are stuck together). Denote by $\mathbf{n} \neq \mathbf{0}$ a vector orthogonal to $\mathbb{X}_i \cap \mathbb{X}_j$ and pointing toward $\mathbb{X}_j$, i.e.,

$$((\mathbf{a} \in \mathbb{X}_i) \wedge (\mathbf{b} \in \mathbb{X}_j)) \Rightarrow \mathbf{n}^{\mathrm{T}} \cdot (\mathbf{b} - \mathbf{a}) \geq 0,$$

then, we have:

$$\begin{array}{lllll} \text{(i)} & ((\forall \mathbf{x} \in \mathbb{X}_i \cap \mathbb{X}_j) & \left(\mathbf{n}^{\mathrm{T}} \cdot \mathbf{f}(\mathbf{x}) > 0\right)) & \Rightarrow & (\mathbb{X}_j \not\hookrightarrow \mathbb{X}_i) \\ \text{(ii)} & ((\exists \mathbf{x} \in \mathbb{X}_i \cap \mathbb{X}_j) & \left(\mathbf{n}^{\mathrm{T}} \cdot \mathbf{f}(\mathbf{x}) > 0\right)) & \Rightarrow & (\mathbb{X}_i \hookrightarrow \mathbb{X}_j). \end{array}$$

Figure 2 illustrates the two conditions (i) and (ii), respectively. In this figure, we have $\dim(\mathbb{X}_i \cap \mathbb{X}_j) = 1$.

**Proof.** Let us first prove (i) by contradiction. Assume that $\mathbb{X}_j \hookrightarrow \mathbb{X}_i$. Then, there exists a trajectory from $\mathbb{X}_j$ to $\mathbb{X}_i$ that crosses $\mathbb{X}_i \cap \mathbb{X}_j$ at a point $\tilde{\mathbf{x}}$. At this point, we have $\mathbf{n}^{\mathrm{T}} \cdot \mathbf{f}(\tilde{\mathbf{x}}) \leq 0$, which is not consistent with the left hand side of (i). To prove (ii), it suffices to take a point $\mathbf{x}_0$ such that $\mathbf{x}_0 \in \mathbb{X}_i \cap \mathbb{X}_j$ and $\mathbf{n}^{\mathrm{T}} \cdot \mathbf{f}(\mathbf{x}_0) > 0$. From (2), we have $\eta(\mathbf{x}_0) = 0$ and $\phi(\eta(\mathbf{x}_0), \mathbf{x}_0) = \mathbf{x}_0 \in \mathbb{X}_j$. Thus, from (3), we get $\mathbb{X}_i \hookrightarrow \mathbb{X}_j$. ■

**Test 2**. Since $\mathbb{X}_i \cap \mathbb{X}_j$ is a polytope, it can be described by linear inequalities, say $\mathbf{A}_{ij} \cdot \mathbf{x} \leq \mathbf{b}_{ij}$. The condition in (i) can be checked by proving the inconsistency of the predicate

$$\left(\mathbf{A}_{ij} \cdot \mathbf{x} \leq \mathbf{b}_{ij}\right) \ \wedge \ \left(\mathbf{n}^{\mathrm{T}} \cdot \mathbf{f}(\mathbf{x}) < 0\right).$$

This can easily be done using interval analysis. A similar reasoning can be done for the condition in (ii).

**Proposition 3.** If the two polytopes $\mathbb{X}_i$ and $\mathbb{X}_j$ do not share, at least partly, a common face, then they are not linked by the relation, i.e.,

$$\dim\left(\mathbb{X}_i \cap \mathbb{X}_j\right) < n-1 \Rightarrow \left(\mathbb{X}_i \not\hookrightarrow \mathbb{X}_j\right).$$

**Proof**. The proof is a direct consequence of (3). ■

**Test 3**. Since $\mathbb{X}_i$ and $\mathbb{X}_j$ are polytopes described by linear inequalities and that are either non-overlapping or equal, Proposition 3 can be tested easily using verified linear programming [7].

**Proposition 4**. Consider a paving $\Omega = \{\mathbb{X}_1, \mathbb{X}_2, \ldots, \mathbb{X}_p\}$. We have

$$\forall j \neq i, \mathbb{X}_i \not\hookrightarrow \mathbb{X}_j \Rightarrow \mathbb{X}_i \hookrightarrow \mathbb{X}_i,$$

which means that if all trajectories starting from $\mathbb{X}_i$ cannot enter inside any of the $\mathbb{X}_j$'s (i.e., $\mathbb{X}_i \not\hookrightarrow \mathbb{X}_j$), then at least one trajectory will stay inside $\mathbb{X}_i$ forever (i.e., $\mathbb{X}_i \not\hookrightarrow \mathbb{X}_i$).

**Proof**. The proof is conducted by contradiction. Assuming that $\mathbb{X}_i \not\hookrightarrow \mathbb{X}_i$, take $\mathbf{x}_0 \in \mathbb{X}_i$. It follows from (3) that the trajectory $\phi\left(t, \mathbf{x}_0\right)$ escapes from $\mathbb{X}_i$ at time $\eta_i\left(\mathbf{x}_0\right)$. Since the paving $\Omega$ covers $\mathbb{R}^n$, $\exists j \neq i$ such that $\phi\left(\eta_i\left(\mathbf{x}_0\right), \mathbf{x}_0\right) \in \mathbb{X}_j$. Or equivalently, $\exists j \neq i, \mathbb{X}_i \hookrightarrow \mathbb{X}_j$, which is inconsistent with the assumption. ■

**Test 4**. Except for atypical situations (such as for instance when one trajectory almost gets out from $\mathbb{X}_i$), the condition of Proposition 4 can be checked easily using interval linear algebra to prove that $\mathbb{X}_i \hookrightarrow \mathbb{X}_i$. The problem is indeed NP-hard [11] in the general case.

The four previous tests can be used to build a quantization of a system described by state equations. The following theorem shows how to deduce an enclosure for the attractor using the associated graph.

**Theorem 1**. Consider a system described by the state equation $\dot{\mathbf{x}} = \mathbf{f}\left(\mathbf{x}\right)$, a paving $\Omega = \{\mathbb{X}_1, \mathbb{X}_2, \ldots, \mathbb{X}_p\}$ of the state space and the graph $\mathcal{G} = (\Omega, \hookrightarrow)$. Define $\Omega^\infty$ as the set of all $\mathbb{X}_i \in \Omega$ of the attractor of $\mathcal{G}$. The set $\Omega^\infty$ (or more precisely the union of the elements it contains) encloses the attractor of the system.

**Proof**. Recall first that the attractor of a directed graph $\Omega$ is the set of all nodes $\mathbb{X}_i$ such that there exists a path from $\mathbb{X}_i$ to $\mathbb{X}_i$. The proof is conducted by contradiction. Take an element $\mathbf{x} \in \mathbb{X}_i \in \Omega$ such that *(i)* $\mathbb{X}_i \notin \Omega^\infty$ and *(ii)* $\mathbf{x}$ belongs to the attractor $\mathbb{A}$ of the dynamical system. Since $\mathbf{x}$ belongs to $\mathbb{A}$, for all $\varepsilon$, there exists $t_1 > 1$ such that $\|\phi\left(t_1, \mathbf{x}\right) - \mathbf{x}\| \leq \varepsilon$. The trajectory crosses the following chain $\mathbb{X}_{i_1}, \ldots \mathbb{X}_{i_m}$, with $\mathbf{x} \in \mathbb{X}_{i_1}$ and $\phi\left(t_1, \mathbf{x}\right) \in \mathbb{X}_{i_m}$. Since $\mathbb{X}_{i_1} \notin \Omega^\infty$ (by assumption), $\mathbb{X}_{i_1} \neq \mathbb{X}_{i_m}$. Since it should be true for all $\varepsilon$, $\mathbf{x}$ should belong to the boundary of $\mathbb{X}_{i_1}$. If it is the case, it means that $\mathbf{x} \in \mathbb{X}_{i_1} \cap \mathbb{X}_{i_m}$,

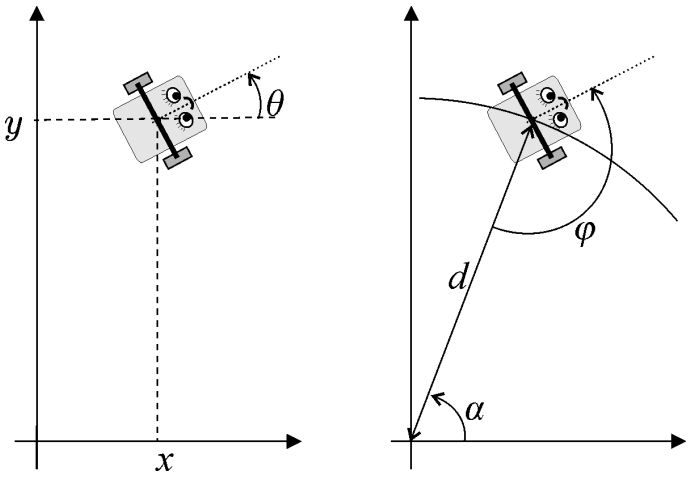


Figure 3: Coordinate transformation for the pose of the robot

and thus there exists a path from $\mathbb{X}_{i_m}$ to $\mathbb{X}_{i_m}$. In such a case, we would have $\mathbf{x} \in \mathbb{X}_{i_m} \in \Omega^\infty$, which is inconsistent with the assumption. ■

From Theorem 1, we are able to compute an enclosure of the attractor of a dynamical system. The procedure that should be followed is the following: (i) build a paving $\Omega = \{\mathbb{X}_1, \mathbb{X}_2, \ldots, \mathbb{X}_p\}$ of the state space $\mathbb{R}^n$, (ii) build the graph $\mathcal{G}$ associated with the relation $\hookrightarrow$, (iii) compute the attractor of the graph, (iv) and return the union of the resulting $\mathbb{X}_i$'s. This will be illustrated in the following section by considering the station keeping problem.

# 3 Station Keeping Problem

The problem of *station keeping* for a robot is to stay inside a disk around origin. Station keeping is needed for instance by sailboat robots [18, 24] that have to anchor inside a delimited area or to stay inside a given corridor [9]. The control problem is known to be difficult, especially in the case of non-holonomous robots [12, 14, 25]. Consider a non-holonomous robot described by the state equations

$$\left\{ \begin{array}{rcl} \dot{x} & = & \cos\theta \\ \dot{y} & = & \sin\theta \\ \dot{\theta} & = & u \ . \end{array} \right.$$

Since $\dot{x}^2 + \dot{y}^2 = 1$, this robot cannot stop. The objective of this robot is to stay inside a zone around zero. Since the problem of controlling the robot has a rotation symmetry, it is possible to describe its relative motion with respect to zero with only two state equations (instead of three). For this, we have to change the coordinates from $(x, y, \theta)$ to $(\alpha, d, \varphi)$, as illustrated by Figure 3. In

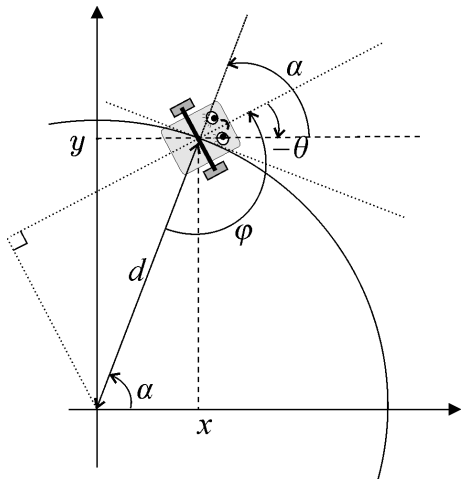


Figure 4: A robot moving around the origin

this figure, $\varphi$ is the heading of the robot with respect to its direction toward zero, $\alpha$ is the azimuth angle and $d$ is its distance to 0.

**Proposition**. The motion of the robot can be described by the state equations

$$\begin{cases} \text{(i)} & \dot{\varphi} &= \frac{\sin\varphi}{d} + u \\ \text{(ii)} & \dot{d} &= -\cos\varphi \\ \text{(iii)} & \dot{\alpha} &= -\frac{\sin\varphi}{d}\ . \end{cases} \tag{4}$$

**Proof**. Proofs for (ii) and (iii) are trivial. To prove (i), from Figure 4, we have

$$\varphi - \theta + \alpha = \pi.$$

Thus, the state equation for the azimuth variable is

$$\dot{\varphi} = -\dot{\alpha} + \dot{\theta} = \frac{\sin\varphi}{d} + u. \quad \blacksquare$$

**Control.** The goal of the *station keeping problem* is to lead and keep the robot around zero, for instance inside a disk. We propose the control

$$u = \begin{cases} +1 & \text{if } \cos\varphi \le \frac{1}{\sqrt{2}} & \text{(the robot turns left)} \\ -\sin\varphi & \text{otherwise} & \text{(the robot goes toward zero)}\ . \end{cases}$$

The idea of this control is to go toward zero using a proportional control if the robot points approximately toward zero (i.e., if $\cos\varphi > \frac{1}{\sqrt{2}}$) and to turn left otherwise. Inserting this control law into state equation (5) yields an autonomous system. The corresponding vector field is not continuous around $\varphi = \pm\frac{\pi}{4}$.

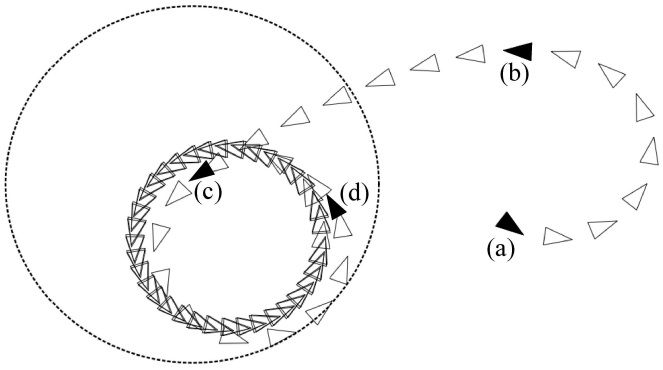


Figure 5: The robot has to stay in a neighbourhood of the origin.

**Summary**. Since the state variable $\alpha$ is not involved in the first two equations of (4), it can be eliminated from the state equations of the robot. In a closed loop form, the motion of the robot can be described by

$$\left\{ \begin{array}{lll} \text{(i)} & \dot{\varphi} & = \left\{ \begin{array}{ll} \frac{\sin\varphi}{d} + 1 & \text{if } \cos\varphi \leq \frac{1}{\sqrt{2}} \\ \left(\frac{1}{d} - 1\right) \sin\varphi & \text{otherwise,} \end{array} \right. \\ \text{(ii)} & \dot{d} & = -\cos\varphi \ . \end{array} \right. \tag{5}$$

Figure 5 provides a simulation of the controlled robot. From its initial state (a), the robot turns left up to state (b). Then, it is controlled by a proportional law. At (c), the robot does no longer points toward zero and turns left again. At state (d), it chooses to go straight for a short period. After that, it stays inside a circle forever.

# 4 Results

Figure 6 represents the vector field of the controlled robot. The trajectory corresponds to the motion depicted on Figure 5. A paving $\mathbb{X}_1, \ldots, \mathbb{X}_6$ is proposed. In a two dimensional case (as here), the paving for the quantization can be deduced directly from a picture of the vector field (which is simple for our example). For higher dimensions, this paving must be done empirically using domain knowledge of the behavior of the dynamical system. We know of no general algorithm able to provide such a significant decomposition (even not validated) in an automatic way. For our example, we explain how we got this quantization.

- *Origin neighborhood*. It corresponds to the box $\mathbb{X}_6$, where the robot is near the point 0. We have no specific strategy inside $\mathbb{X}_6$, and the robot may escape. When the robot is outside $\mathbb{X}_6$, the control tries to bring it back into $\mathbb{X}_6$.

- *Cruising corridor.* Inside $\mathbb{X}_2$ or $\mathbb{X}_5$, the robot navigates toward zero with a proportional control. The heading $\varphi = 0$ is stable, and its distance to zero decreases.

- *Discontinuity corridor.* When the robot is inside $\mathbb{X}_3$, it hesitates between two strategies: to turn left or to go toward the origin. In this corridor, the distance to the origin decreases.

- *Maneuver around the origin.* When the robot is inside the origin neighborhood $\mathbb{X}_6$, it may maneuver, turning left, to go toward the origin. The distance increases, but remains bounded. This corresponds to the set $\mathbb{X}_4$.

- *Maneuver far from the origin.* When the robot is far from the origin neighborhood (inside $\mathbb{X}_1$), it first has to maneuver, turning left, to point toward zero. Then, it will enter inside $\mathbb{X}_2$ and will never come back to $\mathbb{X}_1$.

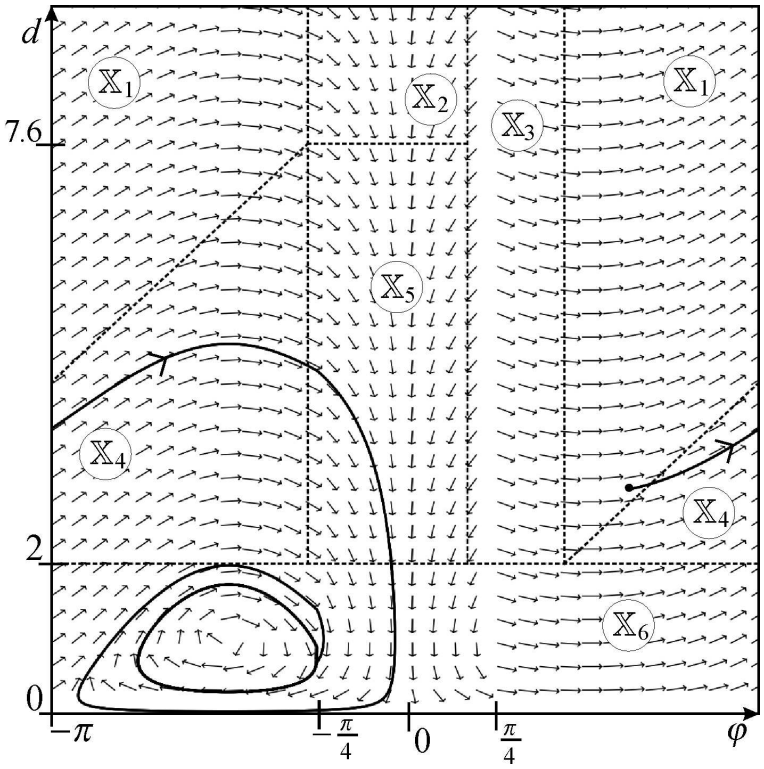


Figure 6: Vector field associated with the station keeping problem. The frame box is $[-\pi, \pi] \times [0, 10]$.

This decomposition is a translation of the reasoning we had when we built our controller. It could have been obtained without visualizing the vector field.

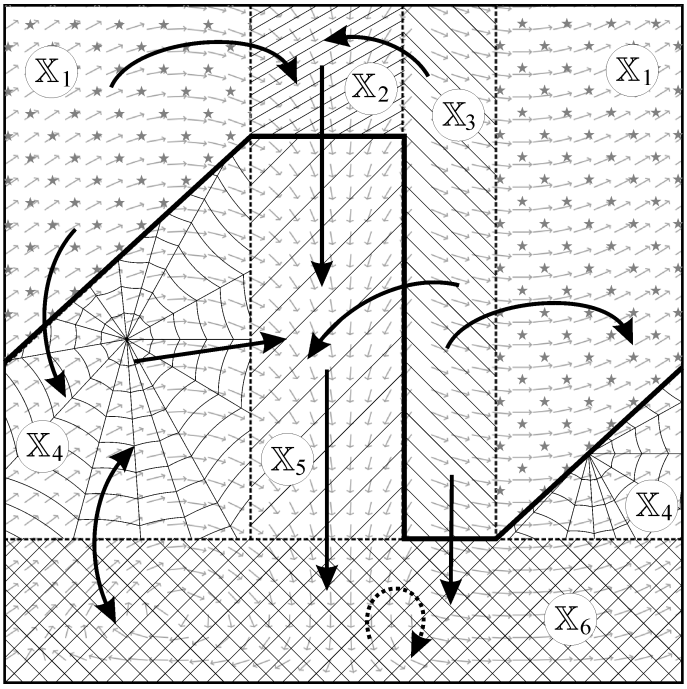


Figure 7: Illustration of the quantization of the state equation

Figure 7 provides the relations we have been able to prove.

**Test 1.** Using Test 1, we have been able to prove that $\mathbb{X}_1 \not\leftrightarrow \mathbb{X}_1$ (take $\mathbf{n} = (1, 0)$), $\mathbb{X}_2 \not\leftrightarrow \mathbb{X}_2$ (take $\mathbf{n} = (0, -1)$), $\mathbb{X}_3 \not\leftrightarrow \mathbb{X}_3$ (take $\mathbf{n} = (0, -1)$), $\mathbb{X}_4 \not\leftrightarrow \mathbb{X}_4$ (take $\mathbf{n} = (1, 0)$) and $\mathbb{X}_5 \not\leftrightarrow \mathbb{X}_5$ (take $\mathbf{n} = (0, -1)$). Test 1 is unable to prove anything about $\mathbb{X}_6$. Of course, from the picture, we guess that $\mathbb{X}_6 \hookrightarrow \mathbb{X}_6$, but none of the four tests is able to prove that.

**Test 2**. Using Test 2, we are able to prove that $\mathbb{X}_1 \overset{\hookrightarrow}{\not\leftarrow} \mathbb{X}_2$, $\mathbb{X}_1 \overset{\hookrightarrow}{\not\leftarrow} \mathbb{X}_4$, $\mathbb{X}_2 \overset{\hookrightarrow}{\not\leftarrow} \mathbb{X}_5$, $\mathbb{X}_3 \overset{\hookrightarrow}{\not\leftarrow} \mathbb{X}_2$, $\mathbb{X}_3 \overset{\hookrightarrow}{\not\leftarrow} \mathbb{X}_1$, $\mathbb{X}_4 \overset{\hookrightarrow}{\not\leftarrow} \mathbb{X}_5$, $\mathbb{X}_5 \overset{\hookrightarrow}{\not\leftarrow} \mathbb{X}_6$, $\mathbb{X}_4 \overset{\hookrightarrow}{\leftarrow} \mathbb{X}_6$, $\mathbb{X}_3 \overset{\hookrightarrow}{\not\leftarrow} \mathbb{X}_6$, $\mathbb{X}_3 \overset{\hookrightarrow}{\not\leftarrow} \mathbb{X}_5$.

**Test 3**. We get $\mathbb{X}_1 \overset{\not\hookrightarrow}{\not\leftarrow} \mathbb{X}_5$, $\mathbb{X}_1 \overset{\not\hookrightarrow}{\not\leftarrow} \mathbb{X}$, $\mathbb{X}_2 \overset{\not\hookrightarrow}{\not\leftarrow} \mathbb{X}_4$, $\mathbb{X}_2 \overset{\not\hookrightarrow}{\not\leftarrow} \mathbb{X}_6$, $\mathbb{X}_3 \overset{\not\hookrightarrow}{\not\leftarrow} \mathbb{X}_4$.

**Test 4.** Since there exists no $\mathbb{X}_i$ such that for $\forall j \neq i$, $\mathbb{X}_i \not\leftrightarrow \mathbb{X}_j$, Test 4 does not apply to our problem, and nothing has been proved about $(\mathbb{X}_6, \mathbb{X}_6)$, even if we could guess that $\mathbb{X}_6 \hookrightarrow \mathbb{X}_6$. Note that Test 4 could apply if we merge $\mathbb{X}_4$, $\mathbb{X}_5$, and $\mathbb{X}_6$ into a single non-convex polytope. Equivalently, since the vector field always enters in the set below the bold broken line of Figure 7, we conclude that $\mathbb{X}_4 \cup \mathbb{X}_5 \cup \mathbb{X}_6$ is a capture basin.

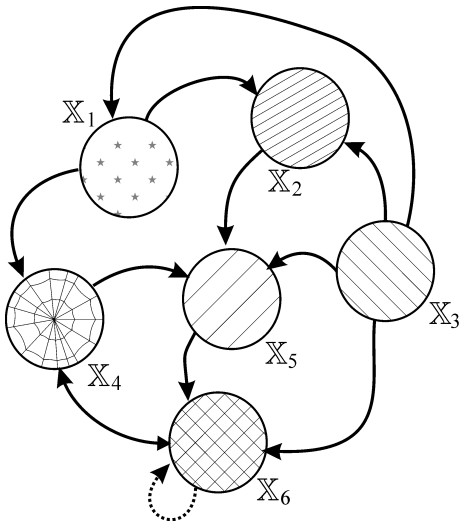


Figure 8: Graph corresponding to the quantization of the state equations

From all tests, the relation $\hookrightarrow$ can be represented in a matrix form by

$$[\mathbf{G}] = \left[\underline{\mathbf{G}}, \overline{\mathbf{G}}\right] = \begin{pmatrix} 0 & 1 & 0 & 1 & 0 & 0 \\ 0 & 0 & 0 & 0 & 1 & 0 \\ 1 & 1 & 0 & 0 & 1 & 1 \\ 0 & 0 & 0 & 0 & 1 & 1 \\ 0 & 0 & 0 & 0 & 0 & 1 \\ 0 & 0 & 0 & 1 & 0 & [0,1] \end{pmatrix},$$

where $[\mathbf{G}]$ is an interval Boolean matrix [10]. The Boolean interval $[0,1]$ in $[\mathbf{G}]$ means that we could have $\mathbb{X}_6 \not\hookrightarrow \mathbb{X}_6$ or $\mathbb{X}_6 \hookrightarrow \mathbb{X}_6$. The single difference between $\underline{\mathbf{G}}$ and $\overline{\mathbf{G}}$ is the $(6,6)$ element which is 0 for $\underline{\mathbf{G}}$ and 1 for $\overline{\mathbf{G}}$. Figure 8 depicts the graph, and the dotted arrow corresponds to the Boolean interval $[0,1]$.

The transitive closure of this graph is

$$\begin{aligned} \left[\mathbf{G}^+\right] &= \left[\underline{\mathbf{G}}^+, \overline{\mathbf{G}}^+\right] = \left[\underline{\mathbf{G}} + \underline{\mathbf{G}}^2 + \underline{\mathbf{G}}^3 + \ldots,\ \overline{\mathbf{G}} + \overline{\mathbf{G}}^2 + \overline{\mathbf{G}}^3 + \ldots\right] \\ &= \begin{pmatrix} 0 & 1 & 0 & 1 & 1 & 1 \\ 0 & 0 & 0 & 1 & 1 & 1 \\ 1 & 1 & 0 & 1 & 1 & 1 \\ 0 & 0 & 0 & 1 & 1 & 1 \\ 0 & 0 & 0 & 1 & 1 & 1 \\ 0 & 0 & 0 & 1 & 1 & 1 \end{pmatrix}, \end{aligned}$$

which is now thin (i.e., with no more interval $[0,1]$). The attractor of the graph is given by the entries equal to 1 in the diagonal of the matrix, corresponding

to the set $\mathbb{X}_4 \cup \mathbb{X}_5 \cup \mathbb{X}_6$. Hence, the attractor of the controlled robot satisfies

$$\mathbb{A} \subset (\mathbb{X}_4 \cup \mathbb{X}_5 \cup \mathbb{X}_6) \ .$$

Thus, we were able to prove that our robot is trapped inside the disk with center 0 and radius $d = 7.6$ (see Figure 6).

# 5 Conclusion

We have proposed an interval-based approach to characterize attractors (or any other limit set) of a dynamical system. We have shown that this can be done without any interval integration and that the paving to be generated should no be made with axis-aligned boxes, but with polytopes instead. The method allows a quantization of the state equation with a paving containing only few elements. This step is necessary to tackle problems with dimensions greater than 5. The paving was built by using a good understanding of the behavior of the system. A next challenging task is to build the paving automatically.

# References

[1] J.P. Aubin and H. Frankowska. *Set-Valued Analysis*. Birkhäuser, Boston, 1990.

[2] M. Berz and K. Makino. Verified Integration of ODEs and Flows using Differential Algebraic Methods on High-Order Taylor Models. *Reliable Computing*, 4(3):361–369, 1998.

[3] P. Collins and A. Goldsztejn. The Reach-and-Evolve Algorithm for Reachability Analysis of Nonlinear Dynamical Systems. *Electronic Notes in Theoretical Computer Science*, (223):87–102, 2008.

[4] E. Cruck, R. Moitie, and N. Seube. Estimation of Basins of Attraction for Uncertain Systems with Affine and Lipschitz Dynamics. *Dynamics and Control*, 11(3):211–227, 2001.

[5] N. Delanoue, L. Jaulin, and B. Cottenceau. Using Interval Arithmetic to Prove that a Set is Path Connected. *Theoretical Computer Science, Special issue: Real Numbers and Computers*, 351(1):119–128, 2006.

[6] A. Goldsztejn, W. Hayes, and P. Collins. Tinkerbell Is Chaotic. *SIAM Journal on Applied Dynamical Systems*, 10(4):1480–1501, 2011.

[7] C. Jansson. Rigorous Lower and Upper Bounds in Linear Programming. *SIAM J. Optim.*, 14(3):914–935, 2004.

[8] L. Jaulin. Path Planning Using Intervals and Graphs. *Reliable Computing*, 7(1):1–15, 2001.

[9] L. Jaulin and F. Le Bars. An Interval Approach for Stability Analysis; Application to Sailboat Robotics. *IEEE Transaction on Robotics*, 27(5), 2012.

[10] L. Jaulin, E. Walter, O. Lévêque, and D. Meizel. Set Inversion for $\chi$-algorithms, with application to guaranteed robot localization. *Mathematics and Computers in Simulation*, 52(3-4):197–210, 2000.

[11] V. Kreinovich, A.V. Lakeyev, and S.I. Noskov. Approximate Linear Algebra is Intractable. *Linear Algebra and its Applications*, 232:45–54, 1996.

[12] L. Lapierre, R. Zapata, and P. Lpinay. Combined Path-following and Obstacle Avoidance Control of a Wheeled Robot. *International Journal of Robotics Research*, 26(4):361–375, 2007.

[13] M. Lhommeau, L. Jaulin, and L. Hardouin. Capture Basin Approximation using Interval Analysis. *International Journal of Adaptative Control and Signal Processing*, 25(3):264–272, 2011.

[14] S. Le Menec. Linear Differential Game with Two Pursuers and One Evader. In M. Breton and K. Szajowski, editors, *Advances in Dynamic Games*, volume 11, pages 209–226, 2011.

[15] R. E. Moore. *Methods and Applications of Interval Analysis*. SIAM, Philadelphia, PA, 1979.

[16] N.S. Nedialkov, K.R. Jackson, and G.F. Corliss. Validated Solutions of Initial Value Problems for Ordinary Differential Equations. *Applied Mathematics and Computation*, 105(1):21–68, 1999.

[17] A. Neumaier. *Interval Methods for Systems of Equations*. Cambridge University Press, Cambridge, UK, 1990.

[18] C. Petres, M. Romero Ramirez, and F. Plumet. Reactive Path Planning for Autonomous Sailboat. In *IEEE International Conference on Advanced Robotics*, pages 1–6, 2011.

[19] J.M. Porta, J. Cortes, L. Ros, and F. Thomas. A Space Decomposition Method for Path Planning of Loop Linkages. In *Proceedings of International Conference on Intelligent Robots and Systems, IROS*, pages 1882–1888, 2007.

[20] N. Ramdani and N. Nedialkov. Computing Reachable Sets for Uncertain Nonlinear Hybrid Systems using Interval Constraint Propagation Techniques. *Nonlinear Analysis: Hybrid Systems*, 5(2):149–162, 2011.

[21] S. Ratschan and Z. She. Safety Verification of Hybrid Systems by Constraint Propagation Based Abstraction Refinement. *ACM Transactions in Embedded Computing Systems*, 6, 2007.

[22] P. Saint-Pierre. Approximation of the Viability Kernel. *Applied Mathematics and Optimization*, 29(2), 1994.

[23] R. Sainudiin. *Machine Interval Experiments: Accounting for the Physical Limits on Empirical and Numerical Resolutions*. LAP Academic Publishers, Kln, Germany, 2010.

[24] C. Sauze and M. Neal. An Autonomous Sailing Robot for Ocean Observation. In *proceedings of TAROS 2006*, pages 190–197, Guildford, UK, 2006.

[25] D. Soetanto, L. Lapierre, and A. Pascoal. Adaptive, Non-Singular Path-Following Control of Dynamic Wheeled Robots. In *IEEE Conference on Decision and Control*, volume 2, pages 1765–1770, 2003.

[26] W. Tucker. The Lorenz Attractor Exists. *Comptes Rendus de l'Acadmie des Sciences*, 328(12):1197–1202, 1999.